Dissociation of cardiomyocyte apoptosis and dedifferentiation in infarct border zones.

European Heart Journal (2002) **23**, 849–857
doi:10.1053/euhj.2001.2963, available online at http://www.idealibrary.com on IDEAL®

Dissociation of cardiomyocyte apoptosis and dedifferentiation in infarct border zones

G. D. Dispersyn[1], L. Mesotten[2], B. Meuris[3], A. Maes[2], L. Mortelmans[2], W. Flameng[3], F. Ramaekers[1] and M. Borgers[1]

[1]*Department of Molecular Cell Biology, Cardiovascular Research Institute Maastricht, Maastricht University, Maastricht, The Netherlands;* [2]*Department of Nuclear Medicine, Gasthuisberg University Hospital, Catholic University Leuven, Leuven, Belgium;* [3]*Centre for Experimental Surgery and Anaesthesiology, Catholic University Leuven, Leuven, Belgium*

Aims Cardiomyocyte apoptosis is known to occur in infarct border zones, where cardiomyocyte dedifferentiation, as seen in hibernating myocardium, can also be observed. The aim of the study is to determine whether dedifferentiated cardiomyocytes represent a population of cells stably surviving or undergoing apoptosis.

Methods and Results Microinfarctions were induced in sheep (n=8) by intracoronary injection of polymer macrobeads. The sheep were killed when cardiac function was gradually decreased (ejection fraction 37 ± 6%, mean ± SEM), but not earlier than 6 weeks after embolization. Transmural biopsies were taken from embolized and remote areas, based on flow measurements with positron emission tomography. Cells were classified as dedifferentiated when sarcomere content was depleted by >10% and glycogen content increased. Apoptosis was detected using the Tdt-mediated nick-end labelling (TUNEL) method and activated caspase-3 immunolabelling. Dedifferentiated cardiomyocytes were identified by morphology and by immunohistochemical evaluation of dedifferentiation related expression patterns of desmin, titin, cardiotin and α-smooth muscle actin. Cardiomyocyte apoptosis was detected in both the infarction border zones and remote areas. Dedifferentiated cardiomyocytes accounted for up to 30% of the cells in embolized areas and were almost exclusively non-apoptotic.

Conclusion In embolization induced microinfarcted tissue, dedifferentiated cardiomyocytes are preferentially spared to undergo apoptosis. It is hypothesized that dedifferentiated cardiomyocytes and apoptotic cardiomyocytes represent two different cell populations. The dedifferentiated cells can be considered as stable surviving cells.
(Eur Heart J 2002; 23: 849–857, doi:10.1053/euhj.2001.2963)

Key Words: Apoptosis, hibernation, myocardial infarction, immunohistochemistry, remodelling.

See page 838 doi:10.1053/euhj.02002.3175 for the Editorial comment on this article

Introduction

It is generally accepted that apoptosis occurs in several cardiac disease states. A well-known paradigm is the occurrence of cardiomyocyte apoptosis in acute pathophysiological conditions, as in acute myocardial infarction. Indeed, in this setting cardiomyocyte apoptosis has been demonstrated in both experimental[1–4] and clinical settings[5–8], and is believed to play an important role in the outcome. Considerable attention has also been paid to the role of apoptosis in more chronic situations and although a causal relationship is far from proven, apoptosis has been consistently linked with heart failure[9–12]. Nevertheless, the role of cell death in more intermediate adaptive processes like chronic hibernating myocardium is still obscure.

Hibernating myocardium was originally described as a protective mechanism of the heart in which it down-regulates its function to cope with oxygen shortage caused by a chronic or repetitive underperfusion accompanied by a limited flow reserve[13–15]. Although hibernating myocardium retains its ability to respond to

Revision submitted 7 August 2001, accepted 15 August 2001, and published online 14 November 2001.

Presented in part at the 73rd Scientific Sessions of the American Heart Association, New Orleans, LA., 12–15 November 2000.

Correspondence: Marcel Borgers, PhD, Department Molecular Cell Biology, CARIM, Maastricht University, Universiteitssingel 50, P.O. Box 616, 6200 MD Maastricht, The Netherlands.

0195-668X/02/110849+09 $35.00/0

inotropic challenges and shows recovery of function after revascularization, this recovery can take a few months to 1 year in a subset of patients with chronic hibernating myocardium[16]. It has been suggested that structural remodelling, which can be found in chronic hibernating myocardium, is at least partially responsible for this delayed recovery of function[17]. These structural changes are characterized by both cellular and extracellular features[18]. It has been shown that the subcellular changes actually represent dedifferentiation of the cardiomyocytes, giving rise to cardiomyocytes with structural hallmarks of fetal heart cells[18,19]. The recovery of function after revascularization is suggestive of the reversibility of the dedifferentiation, although direct evidence is still missing.

Several indirect observations have suggested that dedifferentiated cardiomyocytes represent an adaptive state, enabling the cardiomyocytes to survive under unfavourable circumstances[20]. However, apart from subcellular changes, an increase in the amount of extracellular matrix has also been observed in chronic hibernating myocardium[21,22]. This observation, plus the finding that the recovery of function after revascularization is often incomplete, leaves us with two important questions. First, is cardiomyocyte cell death through apoptosis involved in chronic hibernating myocardium, and secondly, if so, does cardiomyocyte dedifferentiation ultimately lead to cardiomyocyte degeneration? The hitherto limited research into apoptosis in an attempt to answer the first question came up with discrepant findings. Some reported data suggest that apoptosis is an important feature of chronic hibernating myocardium[23,24], while others claim that in this setting apoptosis does not occur, or only to a very limited extent[25].

Two major problems are involved when trying to resolve this issue. First of all, there is the difficulty of accurately detecting low rates of apoptosis which, however, can definitely be of clinical importance after a prolonged period of time[26]. Secondly, especially with regard to the second question, if apoptosis is truly present, then dedifferentiated cardiomyocytes and apoptotic ones might still represent two different cell populations, leaving the possibility that dedifferentiation does not lead to apoptosis per se[27]. In an attempt to answer the latter question, infarct border zones represent a particularly interesting area for investigation. Indeed, it has been shown that in an animal model in which microinfarctions were induced by intracoronary microembolization, not only was cardiomyocyte apoptosis detected but ultrastructural evidence for cardiomyocyte dedifferentiation was also found[10,28]. In the present investigation we used the embolization model to investigate whether cardiomyocyte dedifferentiation and apoptosis could occur in the same or in different cell populations, thereby cataloguing cardiomyocyte dedifferentiation as an adaptive or maladaptive phenomenon. These findings may contribute to answering the clinically important question whether or not patients with hibernating myocardium should undergo revascularization without delay.

Methods

Animal preparation and functional follow-up

In eight juvenile sheep (female, weight 60–65 kg) heart failure was induced by selective intracoronary injection of a suspension of polymer macrobeads, as previously described[29]. In brief, procedures were performed in closed-chest animals by insertion of a Sones catheter into the carotid artery. Injections were given selectively into the left anterior descending (LAD, n=2) or left circumflex (Cx, n=6) coronary artery under fluoroscopic guidance. The embolization solution was prepared by suspending 0·1 g of macrobeads (Bangs Laboratories, Inc., Carmel, Ind., U.S.A.; mean diameter 99 μm) in 5 ml of physiological saline and 5 ml of contrast medium. The mean number of macrobeads in 1 ml suspension was $1{\cdot}85 \times 10^4$. Injection was always followed by severe ECG changes (ST segment elevations) and a drop in arterial blood pressure. All animals underwent transthoracic two-dimensional echocardiography (2D-echo, Sonotron Vingmed CFM 725, Horten, Norway, with 2·5 MHz probe) to assess global and regional myocardial function at baseline, 1 day, 1 week and 6 weeks after the procedure. The measurements were performed on spontaneously breathing animals sedated with ketamine HCl (15–20 mg . kg^{-1} IM). All parameters were measured at the mid-papillary level in the short-axis parasternal view[29]. All echocardiographic measurements were performed by two observers who were blinded to each other's results.

Positron emission tomography

Myocardial blood flow and glucose metabolism were measured with positron emission tomography at 6 weeks after embolization as previously detailed[17]. A whole-body positron emission tomograph (model: ECAT EXACT HR+, CTI Siemens, Knoxville, Tenn.) with 32 detector rings was used. Blood flow was measured using 555 MBq of ^{13}N-ammonia ($^{13}NH_3$). Twenty-two dynamic frames were recorded immediately after injection of the tracer. Total acquisition time was 30 min. The glucose metabolic studies were performed using the hyperinsulinaemic euglycemic clamp technique. Three hundred and seventy MBq of ^{18}F-fluorodeoxyglucose (^{18}FDG) was injected after stabilization of the glucose level between 85 and 95 mg% and 22 dynamic frames were recorded with a total acquisition time 70 min. Both perfusion and metabolic studies were reconstructed and delineated as previously described[17]. The delineation was used to construct a polar map[17]. A region of normal tracer uptake was manually defined on the ammonia polar map. The mean value of that region was used as a reference value, which is 100% ammonia uptake. The same region was used as a reference region on the ^{18}FDG polar map.

In each sheep, two regions of interest were defined on the polar map. The first, representing non-embolized

myocardium, consisted of the area perfused by the non-embolized coronary artery. The second region was drawn over the area perfused by the embolized coronary artery. Flow and metabolic indices were computed for the polar maps. A flow index was calculated as the ratio of $^{13}NH_3$ uptake in the embolized or non-embolized region and as $^{13}NH_3$ uptake in the region with the highest uptake (reference region). A metabolic index was defined as the ratio of glucose utilization in the embolized or the non-embolized region with that in the reference zone.

Tissue processing

Sheep were killed by intravenous injection of saturated KCl after cardiac function was gradually decreased; however, not earlier than 6 weeks after embolization. The whole heart was taken out and different transmural biopsies of the embolized and the non-embolized region were immediately taken, based on the results of the three-dimensional polar map. Using this method, highly accurate myocardial samples could easily be selected from both the affected (embolized) and normal (non-embolized) regions. For immunohistochemistry, tissue samples were immediately frozen in isopentane pre-cooled with liquid nitrogen and stored at −70°C. For the immunohistochemical detection of α-smooth muscle actin, tissue samples were fixed for 20 min in cold (4 °C) 3% glutaraldehyde in 0·09 M KH_2PO_4 (pH 7·4) prior to freezing. For morphological evaluation, tissue samples were fixed in 3% glutaraldehyde, postfixed with 2% OsO_4, dehydrated and embedded in epoxy resin. Semi-thin sections were stained with periodic acid schiff and toluidine blue. Cells were classified as dedifferentiated when the sarcomere content was depleted by >10% and the glycogen content increased.

Immunohistochemistry

For immunohistochemistry, 5 μm frozen sections were cut and stored at −20 °C until use. Apoptosis detection in these sections was performed using the Tdt-mediated nick-end labelling (TUNEL) method and activated caspase-3 detection. The TUNEL method was performed using the Apoptag® peroxidase in situ detection kit (Intergen, Purchase, NY, U.S.A.), following the manufacturer's instructions.

Activated caspase-3 was detected on air-dried frozen sections fixed with 4% paraformaldehyde in phosphate buffered serum. After fixation, the sections were rinsed in phosphate buffered serum and incubated for 1 h in a 0·3 μg . ml^{-1} solution of antiactivated caspase-3 (R&D Systems, Minneapolis, U.S.A.) with 1% bovine serum albumin (BSA) and 0·3% Triton X-100 in phosphate buffered serum. The sections were rinsed in phosphate buffered serum prior to incubation for 45 min with a FITC labelled goat antirabbit antibody (Southern Biotechnology Associates, Birmingham, Alabama, U.S.A.). F-actin was stained using BODIPY® 558/568 phalloidin (Molecular Probes, Leiden, The Netherlands). Nuclei were stained with 0·2 μM TO-PRO®-3 iodide (Molecular Probes). The sections were rinsed and mounted in Slow Fade (molecular probes). For the assessment of cardiomyocyte dedifferentiation, the following monoclonal antibodies were used, which have been described previously[19]: 9D10 against the I-band (at the A-I junction) of titin, RD301 against the tail domain of desmin, R2G against cardiotin, and α-SM-1 (Dako, Glostrup, Denmark) against α-smooth muscle actin. Titin, desmin and cardiotin were labelled using the following procedure: frozen sections were air-dried and then pre-treated with 0·5% Triton X-100 for 5 min, followed by a wash in phosphate buffered serum. Undiluted antisera (with the exception of 9D10: diluted 1:10) were applied on the sections for 1 h. After rinsing in phosphate buffered serum, the sections were incubated for 45 min with a Cy3-labelled goat antimouse antibody (Jackson ImmunoResearch, West Grove, U.S.A.). F-actin was stained using phalloidin-FITC (4 μM, Sigma). The sections were mounted in Slow Fade (Molecular Probes). For the detection of α-smooth muscle actin in frozen glutaraldehyde fixed samples, air-dried frozen sections were treated with 0·5% Triton X-100 for 15 min at room temperature and washed with phosphate buffered serum. After 15-min incubation in 1 mg . ml^{-1} $NaBH_4$ in phosphate buffered serum and pre-incubation in 0·1% bovine serum albumin in phosphate buffered serum, the sections were incubated overnight with the primary antibody at room temperature. After washing with phosphate buffered serum, incubation was performed for 45 min with an alkaline phosphatase conjugated rabbit antimouse Ig (Dako). Vector Blue® (Vector Laboratories Burlingame, U.S.A.) was used to detect alkaline phosphatase activity. The combination of TUNEL and α-smooth muscle detection was performed on frozen glutaraldehyde fixed samples by subsequently following both procedures and postponing the peroxidase and alkaline phosphatase activity detection until the end.

Statistical analysis

Results are given as mean ± SEM. Statistical significance is indicated by P values <0·05. Differences between groups were investigated by using unequal variance t-testing.

Results

Function, flow and metabolism

Embolization induces left ventricular functional changes. Compared with baseline, ejection fraction was

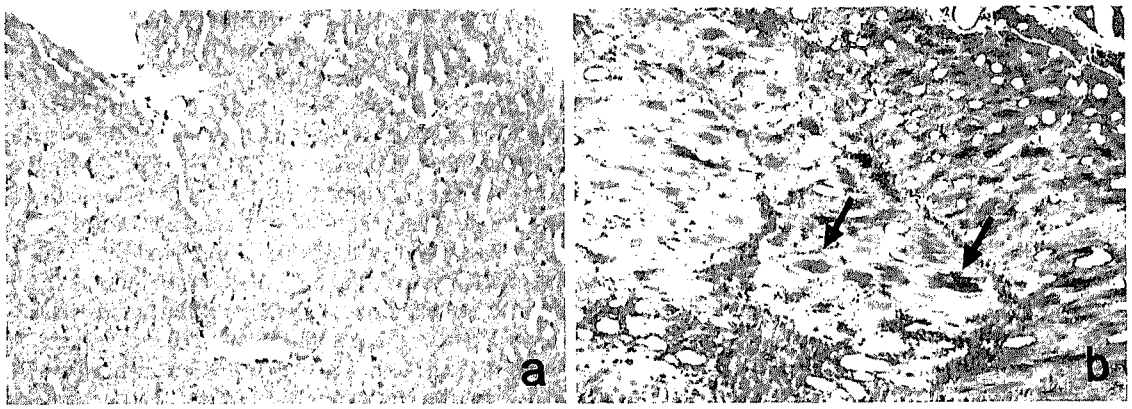

Figure 1 **Light microscopical appearance of periodic acid Schiff and toluidine blue stained sections of microembolized sheep heart. Non-embolized areas (a) were completely normal, whereas embolized regions showed a mix of microinfarcted and viable tissue, the latter being characterized by numerous cardiomyocytes with perinuclear sarcomere depletion and glycogen accumulation (arrows). (a, b: 120 ×).**

significantly but stably decreased 6 weeks after embolization (38% ± 3 vs 69% ± 3). The flow indices and metabolic indices assessed with positron emission tomography imaging were significantly decreased in the embolized areas compared with the non-embolized areas at 6 weeks (74 ± 5% vs 91 ± 2%, $P<0·05$ and 55 ± 5% vs 95 ± 3%, $P<0·05$). Transmural biopsies were taken from embolized (decreased flow and metabolic indices) and non-embolized areas (normal flow and metabolic indices) based on the polar map views.

Morphological evaluation

In the embolized areas, a mix of microinfarcted and viable tissue could be observed, whereas non-embolized areas were devoid of microinfarctions (Fig. 1). In the embolized areas, dedifferentiated cardiomyocytes could be identified and they displayed perinuclear sarcomere depletion and periodic acid Schiff positive glycogen accumulation. These dedifferentiated cardiomyocytes accounted for up to 30% of the cardiomyocyte population in the embolized areas (8 ± 2%), whereas they were virtually absent in non-embolized areas.

Dedifferentiation markers

Immunohistochemical identification of cardiomyocyte dedifferentiation was performed by analysis of protein expression patterns of titin, desmin, cardiotin and α-smooth muscle actin (Fig. 2). In the non-embolized areas all the cardiomyocytes displayed normal, cross-striated patterns of titin and desmin and the normal expression of cardiotin in longitudinal arrays. Desmin was present in large quantities at the intercalated disks. None of these cardiomyocytes expressed α-smooth muscle actin. In the embolized areas, however, abnormal expression patterns could be identified. In cells displaying perinuclear sarcomere depletion (dedifferentiated cardiomyocytes), the normal cross striated patterns of titin and desmin were partially lost. Titin showed, in regions of decreased staining intensity, an unorganized pattern. Desmin showed a mainly perinuclear filamentous pattern in dedifferentiated cells, and was no longer detected at the intercalated disks. Longitudinally oriented cardiotin arrays were less obvious or even completely lost in dedifferentiated cardiomyocytes. Re-expression of α-smooth muscle actin was detected in the dedifferentiated cardiomyocytes of the embolized areas (Fig. 5a).

TUNEL

Analysis of the number of cardiomyocytes showing nuclear DNA fragmentation was performed by TUNEL (Fig. 3). Cardiomyocyte DNA fragmentation was detected in both embolized and non-embolized areas. The number of TUNEL positive cardiomyocytes tended to be higher in the embolized areas compared with the non-embolized areas, but this difference was not statistically significant (0·12 ± 0·04% vs 0·07 ± 0–03, P=ns). In the embolized area, the dedifferentiated cardiomyocytes, recognized by their perinuclear sarcomere depletion, were almost exclusively TUNEL negative and accounted for only 4·9% (representing 2 cells) of the TUNEL positive cardiomyocytes in the embolized areas (Table 1).

Activated caspase-3

Immunohistochemical detection of activated (cleaved) caspase-3 in cardiomyocytes, confirmed the existence of apoptotic cardiomyocytes in both the embolized and non-embolized regions (Fig. 4). Fluorescent labelling of the nuclei with TO-PRO-3[10] showed fragmented nuclei in several instances in both activated caspase-3 cardiomyocytes and interstitial cells (data not shown). The number of activated caspase-3 positive cardiomyocytes in both regions was similar, as found with the TUNEL

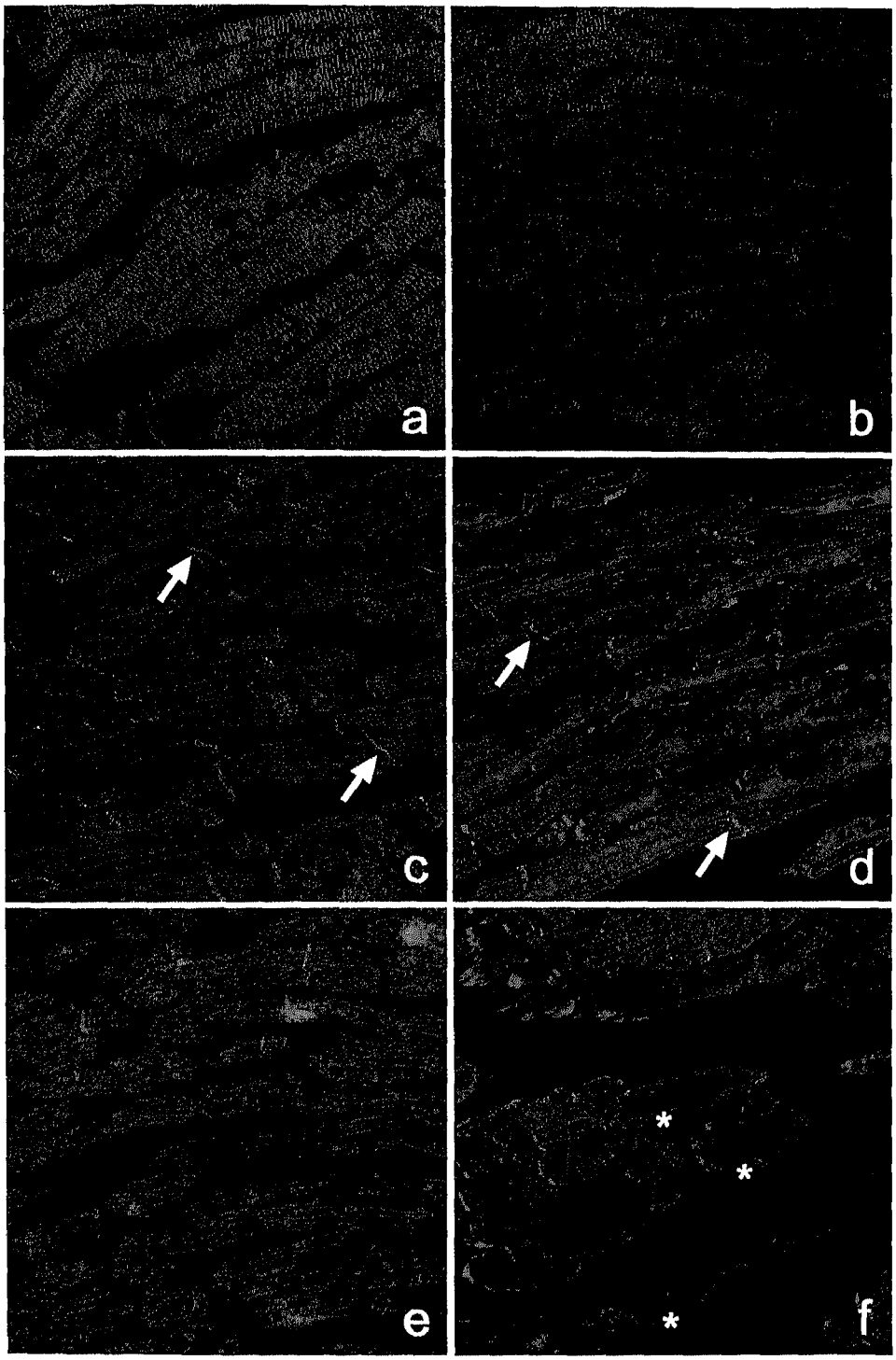

Figure 2 Immunohistochemical detection of protein expression patterns of titin (a, b), desmin (c, d) and cardiotin (e, f) in non-embolized (a, c, e) and embolized (b, d, f) myocardial tissue. In non-embolized regions, titin shows a normal cross striated pattern (a) which, however, is severely lost in dedifferentiated cardiomyocytes in embolized regions (b). Desmin (in red) shows normal cross striations in non-embolized areas, and is present in large amounts at the intercalated disk (colocalization with f-actin stained green with phalloidin — FITC) (c, arrows). In dedifferentiated cells in the embolized areas desmin is no longer detectable at the intercalated disks (no longer a colocalization with f-actin) (d, arrows) and cross striation is partially lost and replaced by a unorganized filamentous pattern, mainly in the perinuclear areas. The normal longitudinally orientated cardiotin arrays (in red) in non-embolized areas (e) can no longer be detected in dedifferentiated cardiomyocytes with perinuclear sarcomere depletion (f, asterisks). (a: 460 × ; b: 440 × ; c: 340 × ; d: 350 × ; e: 340 × ; f: 270 ×).

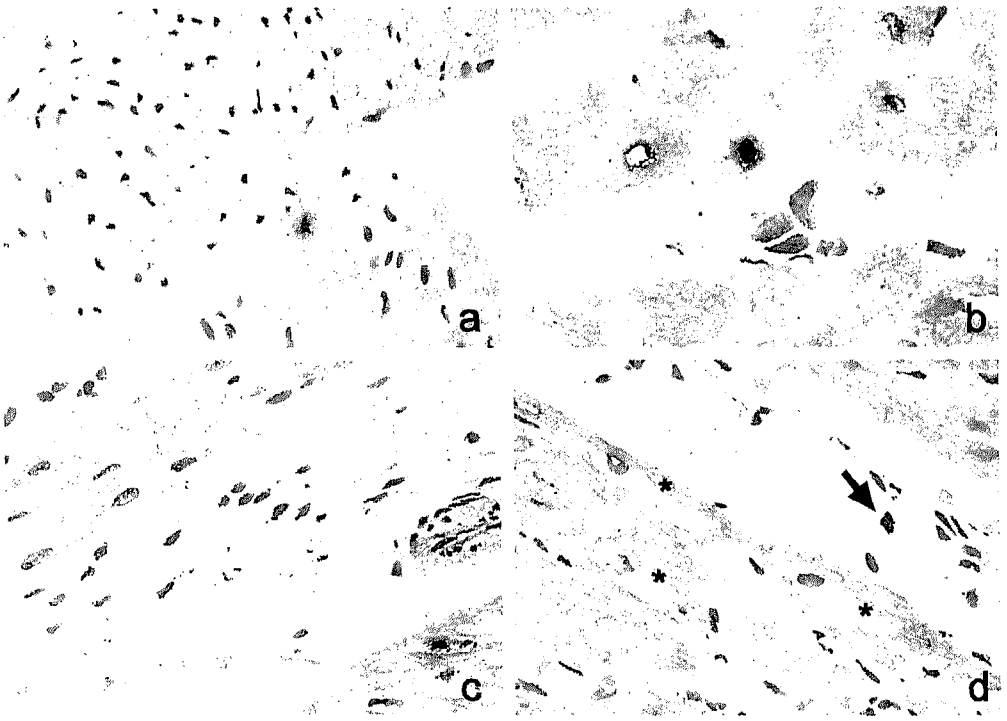

Figure 3 **The TUNEL assay revealed cardiomyocytes with DNA fragmentation (arrows) in both non-embolized (a) and embolized (b) regions. Dedifferentiated cardiomyocytes in the embolized areas, recognized by their perinuclear sarcomere depletion, were — with some exceptions (c, arrow) — almost exclusively TUNEL negative (d, asterisks), although several interstitial cells were positive (d, arrow). (a: 240 × ; b: 480 × ; c: 240 × ; d: 240 ×).**

Table 1 Quantification of the TUNEL positive cardiomyocytes

	TUNEL positive cardiomyocytes				
	Mean ± SEM(%)	Contribution of normal cells		Contribution of dedifferentiated cells	
		Number	%	Number	%
Embolized area	0·12 ± 0·04	39	95·1	2	4·9
Remote area	0·07 ± 0·03	10	100	0	0

method. Again, the difference in the number of activated caspase-3 positive cardiomyocytes between embolized and non-embolized regions was not statistically significant (0·13 ± 0·09% vs 0·04 ± 0·02%, P=ns).

Combined detection of TUNEL and α-smooth muscle action

Since α-smooth muscle actin re-expression is a characteristic feature of cardiomyocyte dedifferentiation, its detection was performed and combined with the assessment of DNA fragmentation to investigate whether or not TUNEL positive cardiomyocytes in embolized areas are dedifferentiated (Fig. 5). We found that none of the α-smooth muscle actin re-expressing cardiomyocytes were TUNEL positive. Conversely, all the TUNEL positive cardiomyocytes were found to be negative for α-smooth muscle actin.

Discussion

In this study we focused on the important question whether degenerative cardiomyocytes and dedifferentiated cardiomyocytes represent the same cell population, i.e. does cardiomyocyte dedifferentiation — as seen in chronic hibernating myocardium — eventually culminate in cell death through apoptosis? This connotation was put forward by Schwarz *et al.*[23], who found evidence for apoptotic cardiomyocytes in patients with chronic hibernating myocardium. In an earlier study, we

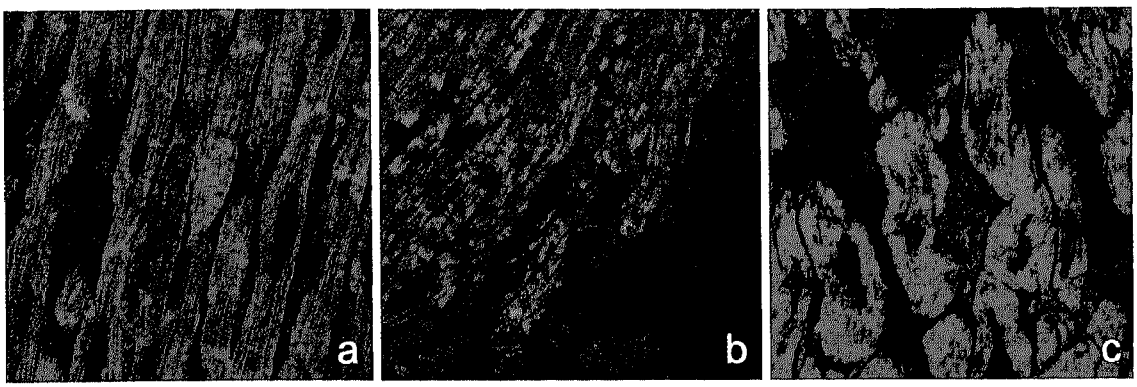

Figure 4 **Immunohistochemical detection of activated caspase-3 in cardiomyocytes. Activated caspase-3 labelling (in green) was seen throughout the cell, in cardiomyocytes in several degrees of deterioration (a through c). (a: 250 × ; b: 385 × ; c: 380 ×).**

Figure 5 **Combined detection of α-smooth muscle actin and DNA fragmentation. A re-expression of α-smooth muscle actin was detected in dedifferentiated cardiomyocytes in the embolized areas (a, in blue). None of these α-smooth muscle actin expressing cardiomyocytes was TUNEL positive. Conversely, all TUNEL positive cardiomyocytes (b, arrow) were negative for α-smooth muscle actin. (a: 240 × ; b: 480 ×).**

were not able to confirm their findings, and concluded that apoptosis in chronic hibernating myocardium, if at all present, would occur to a very limited extent[25]. Tissue is too limited, however, to investigate whether cardiomyocyte dedifferentiation finally leads to apoptosis (needle biopsies from patients with chronic hibernating myocardium). Therefore we used an animal model of microembolization-induced microinfarctions, similar to a model in which it was already shown that cardiomyocyte apoptosis occurs and in which ultrastructural changes suggestive of cardiomyocyte dedifferentiation were found[10,28].

Using immunohistochemical detection of protein expression patterns of different proteins previously investigated in chronic hibernating myocardium[19], we could ascertain that the previously reported ultrastructural changes in viable cardiomyocytes from embolized regions were characteristic of cellular dedifferentiation. The typical changes in the protein expression pattern of titin, desmin, cardiotin and the re-expression of α-smooth muscle actin, were previously reported in patients with chronic hibernating myocardium[19] and a goat model of chronic atrial fibrillation[30], both pathologies in which no evidence for cardiomyocyte apoptosis could be found by us[25]. With regard to hibernating myocardium in patients, failure to detect apoptosis could possibly be attributed to sampling, as it has been shown by Lim *et al.*[31], that apoptosis could be found in a swine model of hibernating myocardium only when a large amount of myocardium was investigated, but not when a a small number of myocytes were investigated with electron microscopy.

In the present study, cardiomyocyte dedifferentiation was only detected in the embolized areas and not in the non-embolized regions. Nevertheless evidence for cardiomyocyte apoptosis could be found in both of these regions, in accordance with a previous investigation[10]. Both the TUNEL method and activated caspase-3 labelling resulted in comparable apoptotic rates. More importantly, however, we found a clear dissociation between TUNEL positive cardiomyocytes and dedifferentiated cardiomyocytes in the embolized regions. With a few exceptions, all of the cardiomyocytes with dedifferentiation hallmarks, like perinuclear sarcomere

depletion (myolysis) and re-expression of α-smooth muscle actin, were TUNEL negative. Aimé-Sempé *et al.*[32], however, reported that almost 50% of the myolytic cardiomyocytes in human chronic fibrillating and dilated right atria, showed TUNEL positive nuclei, suggesting that at least part of these dedifferentiated cardiomyocytes were apoptotic. Nevertheless, the vast majority of these nuclei were enlarged, only weakly stained for TUNEL and DNA ladders and could not be detected, making it more likely that dedifferentiated cardiomyocytes show a high level of transcription. Unfortunately the study did not mention a relationship between Bcl-2, Bax, caspase-3 expression and cellular dedifferentiation hallmarks, although in general they observed a decreased Bcl-2 expression and an increased caspase-3 expression.

The finding of a coexistence of dedifferentiated and degenerated cardiomyocytes in both a dog model of microembolization[10] and in patients with chronic hibernating myocardium (with significant fibrosis)[24] led to the hypothesis that cardiomyocyte dedifferentiation ultimately results in cell degeneration. However, the current findings suggest that cardiomyocyte dedifferentiation and degeneration through apoptosis are not related per se. Indeed, a significant number of apoptotic cardiomyocytes would otherwise be expected in an animal model of chronic atrial fibrillation in which approximately 50% of the cells were found to be dedifferentiated[30]. Nevertheless, no evidence for the occurrence of cardiomyocyte apoptosis could be found in this model[25]. Based on these findings and on the current data, it can be hypothesized that dedifferentiated cardiomyocytes are unlikely to represent a pre-apoptotic state, but instead that dedifferentiated cardiomyocytes and apoptotic ones represent two different cell populations. Moreover, an inverse relationship might be true. It was reported earlier that dedifferentiated cardiomyocytes are more ischaemia tolerant, i.e. better protected against ischaemic insults compared with normally structured cardiomyocytes[20]. Therefore, cardiomyocyte dedifferentiation might be regarded as an adaptive response of the cardiomyocytes to a more unfavourable environment.

With the current data, we cannot unambiguously substantiate this hypothesis: too little apoptotic cardiomyocytes with dedifferentiation hallmarks were found (i.e. two cells) to make a proper statistical analysis, only a rough estimation could be made. It can be estimated that, related to the total amount of dedifferentiated cardiomyocytes, these apoptotic cells account for ca. 0.08%. Although this estimation does not contradict the conclusion that apoptosis and dedifferentiation are not related, it might indicate that dedifferentiated cardiomyocytes are not protected against apoptosis. Further investigations are warranted to address this issue in more detail.

Furthermore, when considering the situation in patients, not only cell survival but also cell function is crucial. Similar to the micro-embolization model, border zones of small infarcts as present in patients may comprise a considerable number of dedifferentiated cells, akin to those in chronic hibernation[18,33]. Although the viability of these cells seems not to be compromised because of the virtual absence of degenerative structural changes, either apoptotic or necrotic, we do not know whether dedifferentiation is reversible after prolonged cell survival. Hence, speedy revascularization is advised in order to subserve the possible redifferentiation of the fetal cardiomyocyte phenotype, which is identical to what has been concluded for chronic hibernating myocardium[16].

In conclusion, we report a dissociation between dedifferentiation and apoptosis in an animal model of microembolization-induced microinfarctions. We show that cardiomyocyte dedifferentiation is not an early stage of a degenerative pathway and can therefore be considered as an adaptation enabling survival of the cells.

This study was in part supported by 'Universiteitsfonds Limburg/SWOL'.

References

[1] Gottlieb RA, Burleson KO, Kloner RA *et al.* Reperfusion injury induces apoptosis in rabbit cardiomyocytes. J Clin Invest 1994; 94: 1621–8.
[2] Cheng W, Kajstura J, Nitahara JA *et al.* Programmed cell death affects the viable myocardium after infarction in rats. Exp Cell Res 1996; 226: 316–27.
[3] Fliss H, Gattinger D. Apoptosis in ischemic and reperfused rat myocardium. Circ Res 1996; 79: 949–56.
[4] Kajstura J, Cheng W, Reiss K *et al.* Apoptotic and necrotic myocyte cell deaths are independent contributing variables of infarct size in rats. Lab Invest 1996; 74: 86–107.
[5] Itoh G, Tamura J, Suzuki M *et al.* DNA fragmentation of human infarcted myocardial cells demonstrated by the nick end labelling method and DNA agarose gel electrophoresis. Am J Pathol 1995; 146: 1325–31.
[6] Misao J, Hayakawa Y, Ohno M *et al.* Expression of bcl-2 protein, an inhibitor of apoptosis, and Bax, an accelerator of apoptosis, in ventricular myocytes of human hearts with myocardial infarction. Circulation 1996; 94: 1506–12.
[7] Olivetti G, Quaini F, Sala R *et al.* Acute myocardial infarction in humans is associated with activation of programmed myocyte cell death in the surviving portion of the heart. J Mol Cell Cardiol 1996; 28: 2005–16.
[8] Saraste A, Pulkki K, Kallajoki M *et al.* Apoptosis in human acute myocardial infarction. Circulation 1997; 95: 320–3.
[9] Narula J, Haider N, Virmani R *et al.* Apoptosis in myocytes in end-stage heart failure. N Engl J Med 1996; 335: 1182–9.
[10] Sharov VG, Sabbah HN, Shimoyama H *et al.* Evidence of cardiocyte apoptosis in myocardium of dogs with chronic heart failure. Am J Pathol 1996; 148: 141–9.
[11] Olivetti G, Abbi R, Quaini F *et al.* Apoptosis in the failing human heart. N Engl J Med 1997; 336: 1131–41.
[12] Guerra S, Leri A, Wang X *et al.* Myocyte death in the failing human heart is gender dependent. Circ Res 1999; 85: 856–66.
[13] Rahimtoola SH. A perspective on the three large multicenter randomized clinical trials of coronary bypass surgery for chronic stable angina. Circulation 1985; 72 (Suppl V): V123–V135.
[14] Rahimtoola SH. The hibernating myocardium. Am Heart J 1989; 117: 211–21.
[15] Braunwald E, Rutherford JD. Reversible ischemic left ventricular dysfunction: evidence for the hibernating myocardium. J Am Coll Cardiol 1986; 8: 1467–70.

[16] Kloner RA, Bolli R, Marban E, Reinlib L, Braunwald E. Medical and cellular implications of stunning, hibernation, and preconditioning: an NHLBI workshop. Circulation 1998; 97: 1848–67.
[17] Maes A, Flameng W, Nuyts J *et al.* Histological alterations in chronically hypoperfused myocardium: correlation with positron emission tomography findings. Circulation 1994; 90: 735–45.
[18] Borgers M, Thone F, Wouters L *et al.* Structural correlates of regional myocardial dysfunction in patients with critical coronary stenosis: chronic hibernation? Cardiovasc Pathol 1993; 2: 237–45.
[19] Ausma J, Schaart G, Thoné F *et al.* Chronic ischemic viable myocardium in man: aspects of dedifferentiation. Cardiovasc Pathol 1995; 4: 29–37.
[20] Ausma J, Thone F, Dispersyn GD *et al.* Dedifferentiated cardiomyocytes from chronic hibernating myocardium are ischemia-tolerant. Mol Cell Biochem 1998; 186: 159–68.
[21] Ausma J, Cleutjens J, Thoné F *et al.* Chronic hibernating myocardium: interstitial changes. Mol Cell Biochem 1995; 147: 35–42.
[22] Elsässer A, Schlepper M, Zimmermann R *et al.* The extracellular matrix in hibernating myocardium — a significant factor causing structural defects and cardiac dysfunction. Mol Cell Biochem 1998; 186: 147–58.
[23] Schwarz ER, Schaper J, vom Dahl J *et al.* Myocyte degeneration and cell death in hibernating human myocardium. J Am Coll Cardiol 1996; 27: 1577–85.
[24] Elsässer A, Schlepper M, Klovekorn WP *et al.* Hibernating myocardium: an incomplete adaptation to ischemia. Circulation 1997; 96: 2920–31.
[25] Dispersyn GD, Ausma J, Thoné F *et al.* Cardiomyocyte remodelling during myocardial hibernation and atrial fibrillation: prelude to apoptosis? Cardiovasc Res 1999; 43: 947–57.
[26] Schaper J, Elsässer A, Kostin S. The role of cell death in heart failure. Circ Res 1999; 85: 867–9.
[27] Dispersyn GD, Borgers M, Flameng W. Apoptosis in chronic hibernating myocardium: sleeping to death? Cardiovasc Res 2000; 45: 696–703.
[28] Sharov VG, Sabbah HN, Ali AS *et al.* Abnormalities of cardiocytes in regions bordering fibrous scars of dogs with heart failure. Int J Cardiol 1997; 60: 273–9.
[29] Zietkiewicz M, Perek B, Meyns B *et al.* Chronic heart failure model induced by coronary embolization in sheep. Int J Artif Organs 1999; 22: 499–504.
[30] Ausma J, Wijffels M, van Eys G *et al.* Dedifferentiation of atrial cardiomyocytes as a result of chronic atrial fibrillation. Am J Pathol 1997; 151: 985–97.
[31] Lim H, Fallavollita JA, Hard R, Kerr CW, Canty JM jr. Profound apoptosis-mediated regional myocyte loss and compensatory hypertrophy in pigs with hibernating myocardium. Circulation 1999; 100: 2380–6.
[32] Aimé-Sempé C, Folliguet T, Rucker-Martin C *et al.* Myocardial cell death in fibrillating and dilated human right atria. J Am Coll Cardiol 1999; 34: 1577–86.
[33] Mesotten L, Maes A, Herregods MC *et al.* PET reduced glucose uptake relative to perfusion pattern early after acute myocardial infarction treated with thrombolytic therapy (abstract). Circulation 2000; 102 (Suppl II): II-770.